

Extracting the QGP viscosity from RHIC data

– a status report from viscous hydrodynamics

Huichao Song and Ulrich Heinz

Department of Physics, The Ohio State University, Columbus, OH 43210, USA

Abstract. We report recent progress on causal viscous hydrodynamics for relativistic heavy ion collisions. For fixed specific shear viscosity η/s , uncertainties in the elliptic flow arising from initial conditions, equation of state, bulk viscosity and numerical viscosity, and the treatment of the highly viscous hadronic stage and freeze-out procedure are analysed. A comparison of current viscous hydrodynamic results with experimental data yields a robust upper limit $\eta/s < 5 \times \frac{1}{4\pi}$.

1. Introduction

The viscosity of the quark-gluon plasma is presently a hotly debated subject. Its computation from first principles is difficult. It is thus desirable to try extracting it from experimental data. Viscous hydrodynamics provides a tool that can be used to attack this problem while simultaneously extending the region of applicability of the hydrodynamic approach beyond that of ideal fluid dynamics.

During the last years, several groups have independently developed (2+1)-dimensional viscous hydrodynamic codes to describe the mid-rapidity spectra from heavy-ion collisions at Relativistic Heavy Ion Collider (RHIC) energies. First results were published in Refs. [1, 2, 3, 4, 5, 6, 7, 8, 9]. It was found that shear viscosity decelerates the longitudinal expansion, thereby initially slowing down the cooling process, but accelerates the transverse expansion, resulting in more radial flow and flatter hadron p_T -spectra. In non-central collisions, the elliptic flow coefficient v_2 was found to be very sensitive to shear viscosity: given the large expansion rates of heavy-ion collision fireballs, even minimal viscosity saturating the KSS bound $\eta/s \geq 1/4\pi$ [10] for the viscosity to entropy density ratio can lead to a strong (and thus easily measurable) suppression of v_2 . Assuming the availability of a well-established ideal fluid dynamical baseline for v_2 as a function of collision energy, centrality and system size, measurements of this suppression could thus be used to constrain the QGP shear viscosity from experimental data. Other observables (e.g. slopes of p_T -spectra) also depend on η/s , but v_2 appears to show the strongest sensitivity, so it has been studied most extensively, and we will focus on it. We will concentrate on viscous hydrodynamics, leaving a discussion of more microscopic approaches (e.g. [11, 12]) for another time.

The first results for viscous v_2 suppression published by the different groups seemed to show large discrepancies, ranging from 20% to 70% for 'minimal viscosity' $\eta/s = 1/4\pi$. A detailed code verification process [13], carried out within the TECHQM collaboration [15], eliminated the possibility that these differences were caused by numerical error. Systematic studies during the last few months revealed their physical origins and are summarized in this talk. Specifically, we will discuss the effects of system size, equation of state (EOS), and different versions of the Israel-Stewart equations used to evolve the viscous terms in the energy-momentum tensor, on viscous v_2 suppression. A combination of these effects has been shown to resolve the

apparent discrepancies reported by different groups [6]. Further, we will discuss effects from different freeze-out procedures [16], different initializations (Glauber model vs. Color Glass Condensate approach) [7], bulk viscosity [17], and numerical viscosity [6]. Quantifying these effects is important for understanding the uncertainties in extracting the shear viscosity to entropy ratio from experimental data.

2. Viscous hydrodynamics in 2+1 dimensions

In this section, we briefly review the causal viscous equations solved by the VISH2+1 code (Viscous Israel-Stewart Hydrodynamics in 2+1 space-time dimensions) developed at OSU, used to simulate QGP and hadronic matter expansion with exact longitudinal boost invariance but arbitrary dynamics in the transverse directions [18]. For simplicity, we assume zero net baryon number and heat conductivity. VISH2+1 solves the equations for energy momentum conservation $d_m T^{mn} = 0$, with

$$T^{mn} = e u^m u^n - (p + \Pi) \Delta^{mn} + \pi^{mn}, \quad \Delta^{mn} = g^{mn} - u^m u^n, \quad (1)$$

together with kinetic equations for the viscous shear pressure tensor π^{mn} and the bulk pressure Π :

$$\Delta^{mr} \Delta^{ns} D \pi_{rs} = -\frac{1}{\tau_\pi} (\pi^{mn} - 2\eta \sigma^{mn}) - \frac{1}{2} \pi^{mn} \frac{\eta T}{\tau_\pi} d_k \left(\frac{\tau_\pi}{\eta T} u^k \right), \quad (2)$$

$$D \Pi = -\frac{1}{\tau_\Pi} (\Pi + \zeta \theta) - \frac{1}{2} \Pi \frac{\zeta T}{\tau_\Pi} d_k \left(\frac{\tau_\Pi}{\zeta T} u^k \right). \quad (3)$$

Here $D = u^m d_m$ is the time derivative in the local comoving frame, $\nabla^m = \Delta^{ml} d_l$ is the spatial gradient in that frame, and $\sigma^{mn} = \nabla^{(m} u^{n)} = \frac{1}{2} (\nabla^m u^n + \nabla^n u^m) - \frac{1}{3} \Delta^{mn} \theta$ (with the scalar expansion rate $\theta \equiv d_k u^k = \nabla_k u^k$) is the symmetric and traceless velocity shear tensor. d_m denotes the components of the covariant derivative in the curvilinear coordinates (τ, x, y, η_s) [18].

For systems with conformal symmetry the last terms in Eqs. (2,3) can be written in different forms as discussed in [6]. While these forms are equivalent for conformal systems, they differ in principle for systems with an EOS that breaks conformal invariance, e.g. through a phase transition. These differences turn out to be negligible in practice [6]. Without the last terms, Eqs. (2,3) are known as *simplified I-S equations* whereas their complete versions will be called *full I-S equations*. In spite of this name, these equations still do not include all possible second-order terms in a gradient expansion around the ideal fluid (locally thermalized) limit. For a conformal theory with vanishing chemical potentials 4 other terms can be added to the right hand side of Eq. (2), with additional coefficients λ_1 , λ_2 , λ_3 , and κ ($\kappa = 0$ in Minkowski space) [19]. These terms include couplings to the vorticity tensor [19] which turns out to be small in heavy-ion collisions if the initial longitudinal velocity profile is boost invariant [1]. Even more terms arise in a kinetic theory derivation that does not assume conformal symmetry [20], including terms that couple Eqs. (2) and (3). Their coefficients can be obtained from kinetic theory [20, 21] at weak coupling or from the AdS/CFT correspondence at strong coupling [19]. Still another approach was developed by Öttinger and Grmela (see references in [3]); when translated into Israel-Stewart form, it also makes specific predictions for the coefficients of these second-order terms [16]. The so far accumulated numerical evidence [6, 7, 13] suggests that, except for the last terms in Eqs. (2) and (3), all other second order terms are unimportant in practice, but a systematic study that confirms this beyond doubt remains outstanding.

The shear viscosity η , bulk viscosity ζ and the corresponding relaxation times τ_π and τ_Π are free parameters in VISH2+1. For most of the published numerical simulations of (2+1)-d viscous hydrodynamics, the shear viscosity has been set to the KSS minimal value $\eta/s = 1/4\pi \simeq 0.08$, and the bulk viscosity was set to zero, $\zeta/s = 0$. Bulk viscous effects on the evolution of elliptic flow in non-central collisions were recently studied by us [17] and are here reported for the first time (see Sec. 5). For the relaxation times τ_π and τ_Π most authors used a constant multiple of η/sT . Physical observables turn out to be largely insensitive to the value of τ_π if (and only if!) the last terms are included in Eqs. (2) and (3), i.e. the *full* (and not the *simplified*!) Israel-Stewart equations are used [6] (see Sec. 3 below).

The equation of state (EOS), initial and final conditions are additional inputs for both ideal and viscous hydrodynamics. Details can be found in the original literature [3, 4, 6, 7] and will not be explained here. Two different EOS will be used in these proceedings: SM-EOS Q is a slightly smoothed version [4] of EOS Q [22] which describes a non-interacting massless QGP phase matched to a chemically equilibrated massive hadron resonance gas (HRG) through a Maxwell construction. EOS L matches the HRG EOS below T_c smoothly with the lattice QCD EOS above T_c [4]. Our EOS L is close to but not identical with the quasiparticle EOS used by Romatschke [1, 7].

3. Viscous v_2 suppression: effects from system size, EOS and different versions of Israel-Stewart equations

In this section we will briefly discuss the different manifestations of shear viscosity when one varies system size and EOS and uses different versions of the I-S equations [6]. As mentioned in the Introduction, this analysis resolves the initially puzzling differences between the results published by different groups.

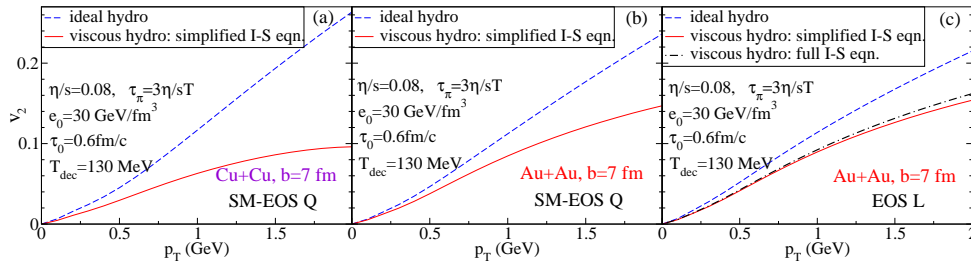


Figure 1. (Color online) Differential elliptic flow $v_2(p_T)$ for directly emitted pions (i.e. without resonance decay contributions), comparing results for different collision systems and EOSs, for ideal and viscous fluid dynamics, with parameters as indicated.

Figure 1 shows the differential elliptic flow $v_2(p_T)$ for directly emitted pions from ideal and viscous hydrodynamics. Panels (a) and (b) compare two systems of different size (Cu+Cu and Au+Au, both at $b = 7$ fm), using the same equation of state (SM-EOS Q), I-S equations (simplified) and other free inputs. Although both systems have similar initial eccentricities, the smaller Cu+Cu system shows a much larger viscous v_2 suppression (by almost 70% below the ideal fluid value at $p_T = 2$ GeV/c [2, 4]) than observed in the larger Au+Au system where the suppression is almost a factor two smaller. Panels (b) and (c) compare the same Au+Au system at $b = 7$ fm for two different EOS SM and different I-S equations. Changing the EOS from SM-EOS Q to

EOS L reduces the viscous suppression of elliptic flow by another quarter (from $\sim 40\%$ to $\sim 30\%$ below the ideal fluid value at $p_T = 2 \text{ GeV}/c$). Replacing the simplified I-S equations used in [2, 4] by the full I-S equations used in [1] further reduces the v_2 suppression from 30% to 25% below the ideal hydrodynamics value at $p_T = 2 \text{ GeV}/c$. This final result is consistent with [1]. Although for EOS L the additional term in the full I-S equations only results in a 5-10% difference in v_2 suppression, its effect is much larger for more rapidly expanding systems, such as Cu+Cu collisions driven by a stiff conformal EOS $e = 3p$ [6]. In such systems the simplified I-S equations lead to a strong sensitivity of physical observables on the value of the microscopic relaxation time τ_π , whereas inclusion of the last term in the full I-S equations (2) appears to minimize this sensitivity in all situations [6]. (It is also needed to preserve the conformal symmetry in conformal systems [19].)

4. Dynamical freeze-out and effects from late hadronic viscosity

In ideal hydrodynamics, one usually imposes “sudden freeze-out”, i.e. a sudden transition from thermalized fluid to free-streaming particles on a hypersurface $\Sigma(x)$ of constant temperature or energy density [22]. The same algorithm has also been used in most of the existing viscous hydrodynamic calculations [1, 2, 4, 5, 6, 7]. Since viscous hydrodynamics is based on an expansion in small deviations from local equilibrium, its validity requires the microscopic relaxation time to be much smaller than the macroscopic inverse expansion rate, $\tau_{\text{rel}}\partial \cdot u \ll 1$. This condition (whose long history is discussed in Ref. [23] where it is also applied to ideal hydrodynamics) provides a natural criterium for a dynamical freeze-out algorithm. Dusling and Teaney [3] implemented it into their viscous hydrodynamics. They find that in this case the viscous v_2 suppression is dominated by non-equilibrium corrections to the local thermal distribution function along the freeze-out surface [3]. This is not a collective effect arising from anisotropies of the flow velocity profile, but a reflection of non-equilibrium momentum anisotropies in the local fluid rest frame. In contrast, for isothermal freeze-out we find [4] that the viscous v_2 suppression is dominated by the viscous reduction of the collective flow anisotropy, while local rest frame momentum anisotropies play a much smaller role. This comparison shows that a careful treatment of the hadronic decoupling process will be required for the quantitative extraction of η/s from elliptic flow data. Dusling also found that dynamical freeze-out can increase the slope of the multiplicity dependence of the eccentricity-scaled elliptic flow v_2/ε [16]. This is an improvement over the scaling behaviour found in [6] for viscous hydrodynamics with constant η/s and isothermal freeze-out which features a slope that is too small.

There are other reasons why a proper kinetic treatment of the late hadronic phase is important. By matching a realistic hadron rescattering cascade to an ideal fluid description of the QGP and hadronization stages, Hirano *et al.* [24] showed that the HRG phase is highly viscous and strongly suppresses any buildup of elliptic flow during the hadronic stage. This is consistent with a recent analysis by Demir and Bass [25] who found large shear viscosities for their hadronic UrQMD cascade even close to T_c (between 5 and 10 times above the KSS bound). For a correct description of the beam energy and centrality dependence of v_2 , which are crucially affected by the changing relative weight of QGP and HRG dynamics in building elliptic flow (in central collisions or at higher energies the system spends more time in the QGP phase than in peripheral collisions or at low energies), a realistic kinetic simulation of the hadronic phase and its freeze-out thus appears to be indispensable. It will

also solve the problem of using an incorrect chemical composition in the hadronic phase that plagues present implementations of viscous hydrodynamics: the empirical finding at RHIC that chemical equilibrium is broken close to T_c and does not (as so far assumed in all viscous codes) persist to the point of kinetic freeze-out has important consequences for elliptic flow. As shown in Refs. [26, 27] within the framework of ideal fluid dynamics, the distribution of the total momentum anisotropy among the various hadronic species depends strongly on the chemical composition of the hadronic fireball at freeze-out, with almost 25% larger pion elliptic flow when chemical equilibrium is broken at $T_c \approx 165$ MeV than for the case where pions are allowed to remain in chemical equilibrium down to $T_{\text{dec}} \approx 100$ MeV. It is obvious that such a large effect must be correctly implemented in viscous hydrodynamics before a quantitative extraction of η/s for the QGP can be attempted.

5. Bulk viscosity

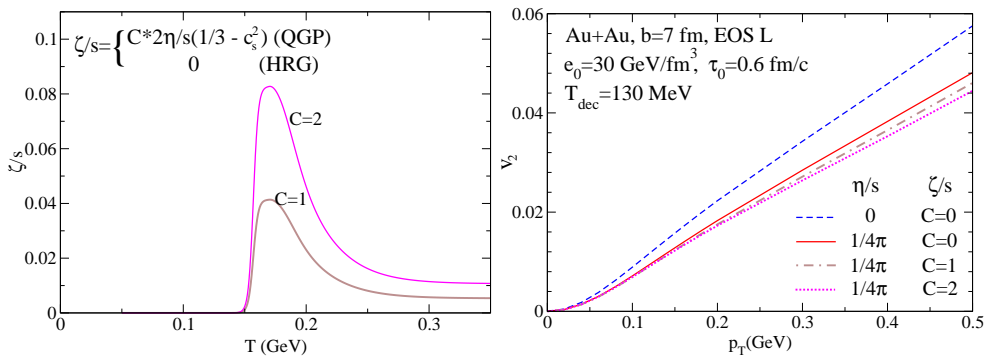


Figure 2. (Color online) *Left:* The bulk viscosity to entropy ratio as a function of temperature, as used in these proceedings (see text for discussion). *Right:* Differential elliptic flow $v_2(p_T)$ for directly emitted pions calculated with ideal hydrodynamics and with viscous hydrodynamics. The viscous calculations assume minimal shear viscosity and three different normalizations of the bulk viscosity shown in the left panel, as noted in the legend.

Early viscous hydrodynamic simulations ignored bulk viscosity for simplicity. Although it vanishes for a conformal fluid or massless QGP on the classical level, quantum effects break the conformal symmetry of QCD and generate a nonzero bulk viscosity even in the massless QGP phase, as recently measured using lattice QCD [28]. General arguments predict that the specific bulk viscosity ζ/s exhibits a peak near T_c [29, 30] and then decreases again on the hadronic side. However, different theoretical approaches show dramatically different peak values: the one from AdS/CFT predictions [31] is more than a order of magnitude smaller than the values extracted from lattice QCD data [28] (see, however, Ref. [32] for a critical discussion of the lattice QCD approach). Considering this theoretical uncertainty, we treat the bulk viscosity as an essentially free input, implementing only the feature that it peaks around T_c . To obtain an explicit expression for $(\zeta/s)(T)$ we connect the minimum AdS/CFT result from Ref. [33], evaluated with lattice QCD data for the speed of sound $c_s^2(T)$, through a Gaussian function peaked at T_c with a zero value in the hadronic phase (lower brown line ($C = 1$) in the left panel of Figure 2). To simulate effects

from larger bulk viscosity, we multiply the entire function by a factor $C > 1$ ($C = 2$ for the upper line in the left panel of Figure 2).

Since the fireball expands, the Navier-Stokes limit of the bulk viscous pressure $\Pi = -\zeta\theta$ is negative. This reduces the thermal pressure (effectively softening the EOS near T_c), decelerates longitudinal expansion and suppresses the buildup of radial flow. As a result, the hadron p_T -spectra become steeper. By construction, the bulk viscous effects are strongest around T_c , but since the transverse edge of the fireball already hadronizes early when the longitudinal expansion rate is high, this does not imply that bulk viscous effects are necessarily small at early times. Indeed, we see in the right panel of Fig. 2 that elliptic flow is significantly reduced by bulk viscosity even though a large fraction of the momentum anisotropy is generated well before most of the matter reaches T_c . For minimal shear viscosity $\eta/s = 1/4\pi$, we find that bulk viscosity can increase the viscous suppression of pion elliptic flow at $p_T = 0.5$ GeV by an additional 25% (for $C = 1$) to 50% (for $C = 2$) relative to the case $\zeta = 0$.

Clearly, bulk viscous effects must be accounted for when trying to extract η/s from elliptic flow data. At this moment it is not clear which observables can be used for a clean separation of bulk and shear viscous effects. One should explore whether the centrality dependence of the local hydrodynamic expansion rate impacts radial and elliptic flow in distinct ways that allow for such a separation.

6. Glauber model vs. CGC initialization

We now come to what may turn out to be a serious road block for precision measurements of the QGP shear viscosity: our insufficient knowledge of the initial source eccentricity ε . It has now been known for while that the Color Glass Condensate (CGC) model, implemented in the initial entropy or energy density profile via the KLN parametrization (see [24, 34] for references), leads to $\sim 30\%$ larger initial source eccentricities than the popular Glauber model. Ideal fluid dynamics transforms this larger source eccentricity into $\sim 30\%$ larger elliptic flow. Since the extraction of η/s is based on the viscous *suppression* of v_2 , obtained by comparing the measured elliptic flow with an ideal (inviscid) fluid dynamical benchmark calculation, a 30% uncertainty in this benchmark can translate into a 100% uncertainty in the extracted value for η/s . This was recently shown by Luzum and Romatschke (see Fig. 8 in [7]). This uncertainty trumps most of the other uncertainties discussed above. Worse, since the initial source eccentricity depends on details of the shape of the KLN profile near the edge of the distribution where the gluon saturation momentum scale Q_s becomes small and the CGC model reaches its limit of applicability, there is little hope that we can eliminate it theoretically from first principles.

Based on their analysis of charged hadron elliptic flow data from the STAR experiment, allowing for a 20% systematic uncertainty of these data, the authors of [7] found an allowed range $0 < \eta/s < 0.1$ for Glauber and $0.08 < \eta/s < 0.2$ for CGC initial conditions. Since their analysis did not include a comprehensive investigation of effects caused by permissible variations of the EOS near T_c , by bulk viscosity, or by late hadronic viscosity and non-equilibrium chemical composition at freeze-out (see Secs. 3 – 5 above), one should add a significant additional uncertainty band to these ranges. Furthermore, correcting the experimental data for event-by-event fluctuations in the initial source eccentricity [35] may bring down the measured v_2 values even below the range considered in [7]. Still, we agree with Luzum and Romatschke that, even when adding all the above effects in magnitude (ignoring the fact that several

of them clearly have opposite signs), viscous hydrodynamics with $\eta/s > 5 \times (1/4\pi)$ would suppress the elliptic flow too much to be incompatible with experiment.

7. Numerical viscosity

To study the effects from shear and bulk viscosity one must ensure that numerical viscosity is under control and sufficiently small. Simply speaking, numerical viscosity comes from the discretization of the hydrodynamic equations for numerical calculation. It causes entropy production even in ideal hydrodynamics without shocks and can never be fully avoided. To minimize numerical viscosity, the flux-corrected transport algorithm SHASTA [36] employed by VISH2+1 (and by its ideal fluid ancestor AZHYDRO [14]) implements an “antidiffusion step” involving a parameter Λ called “antidiffusion constant” [36]. For a given grid spacing, numerical viscosity is maximized by setting $\Lambda = 0$. In standard situations, the default value $\Lambda = \frac{1}{8}$ minimizes numerical viscosity effects [36]. With $\Lambda = \frac{1}{8}$ and typical grid spacing $\Delta x = \Delta y = 0.1$ fm, $\Delta\tau = 0.04$ fm/c, AZHYDRO generates only 0.3% additional entropy in central Au+Au collisions. This is negligible when compared with the $\mathcal{O}(10\%)$ entropy production by VISH2+1 for a fluid with real shear viscosity $\eta/s = 1/4\pi$.

By increasing the grid spacing in AZHYDRO and/or changing Λ , we can explore the effects of numerical viscosity on radial and elliptic flow. We find that numerical viscosity has little effect on the development of radial flow but reduces v_2 in very much the same way as does real shear viscosity. Since we gauge the effects of η/s on v_2 by comparing results from VISH2+1 for $\eta/s \neq 0$ to those for $\eta/s = 0$, we should explore how much in the latter case v_2 is already suppressed by numerical viscosity. We can do this by setting $\eta/s = 0$ and reducing the grid spacing until v_2 stops changing (i.e. until we have completely removed all numerical viscosity effects on v_2). In this way we have ascertained that for our standard grid spacing numerical viscosity suppresses the differential elliptic flow $v_2(p_T)$ by less than 2%.

8. Summary and outlook

While the elliptic flow v_2 generated in non-central heavy-ion collisions is very sensitive to the shear viscosity to entropy ratio η/s of the QGP, it is also significantly affected by (i) details of the initialization of the hydrodynamic evolution, (ii) bulk viscosity and sound speed near the quark-hadron phase transition, and (iii) the chemical composition and non-equilibrium kinetics during the late hadronic stage. Not all of these effects are presently fully under control. Recent attempts to extract the specific shear viscosity η/s phenomenologically, by comparing experimental elliptic flow data with viscous hydrodynamics, have established a robust upper limit

$$\left. \frac{\eta}{s} \right|_{\text{QGP}} < 5 \times \frac{1}{4\pi}, \quad (4)$$

close to the conjectured KSS bound [10], but further progress requires elimination of the above systematic uncertainties. Since some of these influence the build-up of elliptic flow in opposite directions, it is quite conceivable that the QGP specific viscosity is in fact much closer to the KSS bound $(\eta/s)|_{\text{KSS}} = 1/4\pi$ than suggested by the upper limit (4). Ongoing improvements on the theory side should help to reduce or eliminate most of the above uncertainties, bringing us closer to a quantitative extraction of η/s for the quark-gluon plasma. The single largest uncertainty, however, is caused by our poor knowledge of the initial source eccentricity which varies by about

30% between models. As shown in [7], this translates into an $\mathcal{O}(100\%)$ uncertainty for η/s . It seems unlikely that theory can help to eliminate this uncertainty from first principles. It thus appears crucial to develop experimental techniques that may help us to pin down the initial source eccentricity phenomenologically, with quantitative precision at the percent level.

Acknowledgments:

We thank K. Dusling, R. Fries, P. Huovinen, M. Lisa, P. Petreczky, and X.-N. Wang for fruitful discussions. This work was supported by the U.S. Department of Energy under grant DE-FG02-01ER41190.

References

- [1] Romatschke P and Romatschke U 2007 *Phys. Rev. Lett.* **99** 172301
- [2] Song H and Heinz U 2008a *Phys. Lett. B* **658** 279
- [3] Dusling K and Teaney D 2008 *Phys. Rev. C* **77** 034905
- [4] Song H and Heinz U 2008b *Phys. Rev. C* **77** 064901
- [5] Chaudhuri A K 2008 arXiv:0801.3180 [nucl-th]
- [6] Song H and Heinz U 2008c *Phys. Rev. C* **78** 024902
- [7] Luzum M and Romatschke P 2008 *Phys. Rev. C* **78** 034915
- [8] Molnar D and Huovinen P 2008 *J. Phys. G: Nucl. Part. Phys.* **35** 104125
- [9] Heinz U and Song H, *J. Phys. G: Nucl. Part. Phys.* **35** 104126
- [10] Kovtun P, Son D T and Starinets A O 2005 *Phys. Rev. Lett.* **94** 111601
- [11] Xu Z and Greiner C 2005 *Phys. Rev. C* **71** 064901; Xu Z and Greiner C 2007 *Phys. Rev. C* **76** 024911; Xu Z, Greiner C and Stöcker H 2008 *Phys. Rev. Lett.* **101** 082302; Xu Z and Greiner C 2008 *Preprint* arXiv:0811.2940 [hep-ph].
- [12] Huovinen P and Molnar D 2008 *Preprint* arXiv:0808.0953 [nucl-th].
- [13] At the end of 2007, a partial code verification was performed by P. Romatschke and one of us (H.S) between the code UVH2+1 [14] used in [1, 7] and our VISH2+1 code [2, 4, 6]. A more detailed verification was done in 2008 by K. Dusling and H.S. between VISH2+1 and the Stony Brook code [3] (the latter is based on the slightly different Öttinger-Grmela formalism). A preliminary documentation of the test results, which show excellent agreement, can be found on the TECHQM web site [15]; a publication is in preparation.
- [14] UVH2+1 and AZHYDR0 can be downloaded from URL <http://karman.physics.purdue.edu/OSCAR/>
- [15] https://wiki.bnl.gov/TECHQM/index.php/Code_verification_for_viscous_hydrodynamics
- [16] Dusling K 2008 private communication
- [17] Song H and Heinz U 2009 manuscript in preparation
- [18] Heinz U, Song H and Chaudhuri A K 2006 *Phys. Rev. C* **73** 034904
- [19] Baier R, Romatschke P, Son D T, Starinets A O and Stephanov M A 2008 *JHEP* **0804** 100
- [20] Betz B, Henkel D and Rischke D H 2008 arXiv:0812.1440 [nucl-th]
- [21] York M A and Moore G D 2008 arXiv:0811.0729 [hep-ph]
- [22] Huovinen P 2004 in *Quark Gluon Plasma 3*, edited by R. C. Hwa and X. N. Wang (World Scientific, Singapore), p. 600 [arXiv:nucl-th/0305064]; Kolb P F and Heinz U 2004 *ibid.*, p. 634 [arXiv:nucl-th/0305084]
- [23] Heinz U and Kestin G 2008 *Eur. Phys. J. Special Topics* **155** 75
- [24] Hirano T, Heinz U, Kharzeev D, Lacey R and Nara Y 2006 *Phys. Lett. B* **636** 299
- [25] Demir N and Bass S A 2008 arXiv:0812.2422 [nucl-th]
- [26] Hirano T and Tsuda K 2002 *Phys. Rev. C* **66** 054905
- [27] Kolb P F and Rapp R 2003 *Phys. Rev. C* **67** 044903
- [28] Meyer H B 2008 *Phys. Rev. Lett.* **100** 162001
- [29] Paech K and Pratt S 2006 *Phys. Rev. C* **74** 014901;
- [30] Karsch F, Kharzeev D and Tuchin K 2008 *Phys. Lett. B* **663** 217
- [31] Gubser S S, Nellore A, Pufu S S and Rocha F D 2008 *Phys. Rev. Lett.* **101** 131601
- [32] Moore G D and Saremi O 2008 *JHEP* **0809** 015
- [33] Buchel A 2008 *Phys. Lett. B* **663** 286
- [34] Drescher H J, Dumitru A, Hayashigaki A and Nara Y 2006 *Phys. Rev. C* **74** 044905
- [35] Poskanzer A 2008 private communication
- [36] Boris J P and Book D L 1973 *J. Comput. Phys.* **11** 38